Linking tree-ring growth and satellite-derived gross primary growth in multiple forest biomes. Temporal-scale matters

Sergio M. Vicente-Serrano[1]*, Natalia Martín-Hernández[1], J. Julio Camarero[1], Antonio Gazol[1], Raúl Sánchez-Salguero[1,2], Marina Peña-Gallardo[1], Ahmed El Kenawy[1,3], Fernando Domínguez-Castro[1], Miquel Tomas-Burguera[4], Emilia Gutiérrez[5], Martin de Luis[6], Gabriel Sangüesa-Barreda[1,8], Klemen Novak[6,7], Vicente Rozas[8], Pedro A. Tíscar[9], Juan C. Linares[2], Edurne Martínez del Castillo[6], Montse Ribas[5], Ignacio García-González[10], Fernando Silla[11], Alvaro Camisón[12], Mar Génova[13], José M. Olano[8], Luis A. Longares[6], Andrea Hevia[14,15], J. Diego Galván[16]

[1]Instituto Pirenaico de Ecología (IPE-CSIC), 50059 Zaragoza, Spain. [2]Depto. Sistemas Físicos, Químicos y Naturales, Univ. Pablo de Olavide, 41013 Sevilla, Spain. [3] Department of Geography, Mansoura University, Mansoura, 35516, Egypt. [4]Estación Experimental Aula Dei, Consejo Superior de Investigaciones Científicas (EEAD-CSIC), 50192 Zaragoza, Spain. [5]Dept. Evolutionary Biology, Ecology and Environmental Sciences, Univ. Barcelona, 08028 Barcelona, Spain. [6]Depto. Geografía y Ordenación del Territorio - IUCA, Univ. Zaragoza, 50009 Zaragoza, Spain. [7]Depto. de Ecología, Universidad de Alicante, Carretera San Vicente del Raspeig s/n, 03080 San Vicente del Raspeig, Alicante, Spain. [8] Dept. CC. Agroforestales, iuFOR-EiFAB, Univ. Valladolid, 42004 Soria, Spain. [9]Centro de Capacitación y Experimentación Forestal. C/. Vadillo-Castril. 23470 Cazorla, Spain. [10]Depto. Botánica, Escola Politécnica Superior, Campus Terra, Univ. Santiago de Compostela, 27002 Lugo, Spain. [11]Depto. Biología Animal, Parasitología, Ecología, Edafología y Química Agrícola, Univ. Salamanca, 37071 Salamanca, Spain. [12]Ingeniería Forestal y del Medio Natural, Univ. Extremadura, 10600 Plasencia, Spain. [13]Depto. Sistemas y Recursos Naturales, Univ. Politécnica de Madrid, 28040 Madrid, Spain, [14]Forest and Wood Technology Research Centre (CETEMAS), 33936, Siero, Asturias, Spain. [15]Depto. Ciencias Agroforestales, Univ. Huelva, Escuela Técnica Superior de Ingeniería, Campus La Rábida, Palos de la Frontera, 21819 Huelva, Spain. [16]Ionplus AG. Lerzenstrasse 12, 8953 Dietikon, Switzerland.

Abstract

This study links tree-ring growth and gross primary production for a variety of forest types under different environmental conditions across Spain. NOAA-AVHRR satellite imagery data were combined with dendrochronological records and climate data at a fine spatial resolution (1.21 km^2) to analyze the interannual variability of tree-ring growth and vegetation activity for different forest biomes from 1981 to 2015. Specifically, we assessed the links between tree-ring width indices (TRWi), the Normalized Difference Vegetation Index (NDVI) and a variety of environmental conditions, represented by climatic variables (air temperature, precipitation, evapotranspiration and water balance) and elevation. The impact of these variables on tree growth was assessed by means

of the Predictive Discriminant Analysis (PDA). Results reveal a general positive and significant relationship between inter-annual variability of the NDVI at a high spatial resolution (1.21 km^2) and tree-ring growth. Maximum correlations between NDVI and tree-ring growth were recorded when cumulative NDVI values were considered, in some cases covering long time periods (6-10 months), suggesting that tree growth is mainly related to Gross Primary Production (GPP) at annual scale. The relationship between tree-ring growth and inter-annual variability of the NDVI, however, strongly varies between forest types and environmental conditions.

Key-words: vegetation activity, normalized difference vegetation index, annual tree-ring, forest growth, climate, Spain.

1. Introduction

Climate plays a paramount role, controlling the inter-annual variability of both gross primary production (GPP) and secondary growth of trees (Barber et al., 2000; Ciais et al., 2005; Lundqvist et al., 2018; Nemani et al., 2003; Olson et al., 2018; Rubio-Cuadrado et al., 2018). Under a changing climate scenario, the impacts of climate change related extreme events (e.g. droughts, heat waves) on tree growth appear as a main concern. Numerous studies have confirmed climate influence on forest GPP (e.g. Granier et al., 2007; Zhao and Running, 2010) and tree secondary growth as well (Camarero et al., 2015; Orwig and Abrams, 1997; Rötzer et al., 2012; Vicente-Serrano et al., 2014). Nevertheless, the response of vegetation activity, as regards GPP and secondary growth, to climate variability can differ significantly over contrasting forest biomes, as a function of regional-scale climate characteristics, land cover, topographical gradient, etc. (Bhuyan et al., 2017; Gazol et al., 2018; Montserrat-Martí et al., 2009; Tognetti et al., 2007).

Growth and productivity can differ among populations of the same tree species living under different climate conditions (Peguero-Pina et al., 2007). For example, del Castillo et al. (2015)

63 indicated that leaf activity and radial growth of the Aleppo pines have different response patterns to
64 precipitation in eastern Spain. More recently, Gazol et al. (2018) confirmed that the resilience of
65 forests to the occurrence of drought events in Spain is different considering leaf activity or tree-ring
66 growth. As such, it is important to assess the possible links between climate determinants and GPP
67 and secondary tree growth. This assessment is also desired for a better understanding of the
68 influence of different projected scenarios of climate change on forest growth and productivity
69 (Sánchez-Salguero et al., 2017).

70 Nonetheless, as opposed to the long-term time-series of secondary growth of trees obtained
71 using dendrochronological techniques (Grissino-Mayer and Fritts, 1997), long-term measurements
72 of GPP are not widely available. This temporal inconsistency makes it difficult to directly assess the
73 relationship between GPP and secondary growth across different biomes. However, with the
74 advancement in remote sensing instruments and techniques, vegetation information derived from
75 different satellite platforms, which extends back to the early 1980s, can be a valuable resource as a
76 reliable surrogate for GPP primary production data of trees. Specifically, different vegetation
77 indices can be calculated with spectral radiometric information. On one hand, these indices are
78 closely related to different vegetation features, while they can give indications on the trees' primary
79 above-ground productivity on the other hand. Among all these indices, the most common is the
80 Normalized Difference Vegetation Index (NDVI), which shows strong relationship with
81 photosynthetically active radiation (Myneni et al., 1995), the leaf area index (Baret and Guyot,
82 1991; Carlson and Ripley, 1997) and the total green biomass (Cihlar et al., 1991; Gutman, 1991;
83 Tucker et al., 1983; Wylie et al., 2002). The NDVI has widely been used for several purposes,
84 including the analysis of vegetation trends (Herrmann et al., 2005; Zhou et al., 2001) and their
85 relationships with climate variability and droughts (Kogan, 1997; Vicente-Serrano, 2007).

86 Several studies have used NDVI data as key input in net primary production (NPP) models
87 because of their relationship (e.g., Nemani et al., 2003; Zhao and Running, 2010), but NDVI is not a

direct metric of the NPP. What the NDVI really represents is the gross primary production (GPP); in other words the vegetation photosynthetic activity or the photosynthetically active radiation obtained by vegetation (Myneni et al., 1995). Part of this energy obtained by vegetation is consumed in respiration processes, and the remaining is the NPP, which includes the primary and secondary growth but also flowers, fruits, etc. Tree-ring growth can be considered a good integrating variable (Grissino-Mayer and Fritts, 1997). Therefore, the NDVI can be employed to assess the possible links between primary production and secondary forest growth variability (Kaufmann et al., 2008; Vicente-Serrano et al., 2016; Pasho and Alla, 2015).

Current available datasets of NDVI cover in some cases, more than 30 years of time (e.g. Pinzon and Tucker, 2014). This allows combining NDVI, as a proxy of primary productivity, with tree-ring width series. In this context, several studies have already found positive and significant relationships between NDVI and radial secondary growth (tree-ring width) across different forest types worldwide (e.g. Alla et al., 2017; Coulthard et al., 2017; Leavitt et al., 2008; Liang et al., 2009; Lopatin et al., 2006; Malmström et al., 1997). Nonetheless, these relationships are complex and varies widely across different climate regions, forest types and biomes (Bhuyan et al., 2017; Gazol et al., 2018) and they are characterized by contrasting responses according to the period of the year in which NDVI is recorded and averaged (Vicente-Serrano et al., 2016). According to Gough et al. (2008), the cumulative NDVI values over determined periods can be seen as better proxies of the total NPP, which strongly determines secondary growth.

The existing studies focusing on the links between NDVI and secondary growth are usually based on the Global Inventory Monitoring and Mapping Studies (GIMMS) dataset, which is the key reference for temporally homogeneous global NDVI datasets (Pinzon and Tucker, 2014; Tucker et al., 2005). Nonetheless, the utility of the GIMMS NDVI is mainly constrained by its very low spatial resolution (ca. 8 km). While this low spatial resolution may not be critical in boreal homogeneous landscapes, given that the same forest can dominate over large areas, this resolution

113 remains questionable in more heterogeneous areas, hindering the comparison between GIMMS
114 NDVI and site tree-ring width series. These limitations increase with increasing landscape
115 complexity. A good example is Mediterranean-type ecosystems, where vegetation exhibits strong
116 spatial heterogeneity. The global patterns of response of tree-ring growth to NDVI time-scales,
117 described in Vicente-Serrano et al. (2016), cannot be completely representative of the highly-
118 diverse Mediterranean region.

119 The aim was to analyze the relationships between NDVI and tree-ring width series, as
120 reliable proxies of primary production and secondary growth, respectively. To accomplish this task,
121 we employed a very dense network of tree-ring width chronologies (n = 566 forests), covering 16
122 dominant forest tree species. This dataset comprised the diverse climatic and environmental
123 conditions found across the Spanish Peninsula and the Balearic islands. Our specific objectives
124 were: i) to determine the relationships between NDVI and tree-ring width for different tree species
125 representing different forest biomes in Spain, and ii) to assess the relative contribution of tree
126 species and environmental conditions to the different patterns of relationships observed between
127 NDVI and tree-ring width.

128

129 **2. Material and methods**

130 *2.1. Normalized Difference Vegetation Index (NDVI) dataset*

131 We employed a recently developed high (1.21 km^2) spatial resolution NDVI dataset, spanning the
132 entire Spanish peninsula and the Balearic Islands. This dataset was developed using daily afternoon
133 passes of the NOAA-AVHRR images from 1981 to 2015. These images were subjected to a
134 complete calibration, quality control, geometric matching, cloud removal and topographic
135 correction. After the calculation of the NDVI, the daily images were aggregated into semi-monthly
136 composites by means of the Maximum Value Composite (MVC) technique. The images were also
137 filtered to reduce the presence of noise associated with the processing method. The quality and

accuracy of this dataset was verified, given its strong temporal coherence in comparison to the GIMMS dataset, but with a higher spatial resolution. Further details about the processing and characteristics of the NDVI dataset are outlined in Martín-Hernández et al. (2017).

2.2. Tree-ring dataset

We used tree-ring width data obtained using dendroecologic methods and covering most of the forests in the Spanish Peninsula and the Balearic Islands (Figure 1). The forest sampling was not specifically designed for this research so we used forest samples collected by a number of research teams in Spain during the last two decades. The available samples are comparable since they used standard and common criteria when they were collected in the field. For each forest, a minimum number of 10-15 apparently healthy and dominant or codominant trees were selected and cored at 1.3 m using Pressler increment borers to extract 2-3 cores per tree, usually samples perpendicular to the maximum slope. For each studied stand, geographical coordinates (latitude, longitude) and elevation were recorded. Wood cores were carefully sanded to facilitate the estimation of rings and then then these samples were visually cross-dated. After that, using binocular microscopes and tree-ring measurement devices (Lintab, F. RinnTech., Germany; Velmex Inc., USA), tree-ring width was measured with a 0.01 mm resolution. COFECHA (Holmes, 1983) was used to check the accuracy of visual cross-dating and measurements. This procedure calculates moving correlations between each individual tree-ring series and the mean site series to check the visual cross-dating.

Tree-ring width measurements were converted into residual ring-width indices (Fritts, 1976). First, the individual series of tree-ring widths were detrended using a negative exponential curve and residuals were obtained by dividing the observed values by the fitted ones. Second, the individual standardized series were averaged into site mean or master chronologies of tree-ring width indices (hereafter TRWi) using bi-weight robust means to reduce the effects of outliers. The mean site-level or master chronology reflects the year-to-year variability in radial growth of a

variable number of trees of the same species growing at the same forest (see Table 1). The detrending process allowed removing the low- to mid-frequency variability, while keeping the high-frequency variability and the first-order autocorrelation since no autoregressive model was fitted to the TRWi. The species with a higher number of sampled forests were *Pinus halepensis* (117 forests), followed by *Pinus sylvestris* (76) and *Pinus nigra* (66). The most intensively sampled hardwood species were: *Fagus sylvatica* (51), *Castanea sativa* (10), and *Quercus* species. The location of the sampled forests is shown found in Figure S1.

2.3. Methodology of combining NDVI And TRWi

2.3.1. Patterns and relationships between NDVI and tree-ring width series

The NDVI data can be affected by trends in the time series as a consequence of different factors including CO_2 fertilization (Donohue et al., 2013), and forest densification (Vicente-Serrano et al., 2004). For this reason, and to be comparable with the available de-trended tree-ring series, we proceeded to detrend the semi-monthly NDVI. For this purpose we used a linear regression analysis to fit NDVI (dependent variable) with time (independent variable). The residuals of the model were summed to the average of the entire semi-monthly period to have detrended NDVI series. To quantify the NDVI-TRWi associations, we calculated Pearson correlation coefficient between the annual TRWi and the detrended semi-monthly NDVI series at each forest site. Since the cumulative NPP over long periods can give better estimations of tree-ring width than that of shorter periods (Gough et al., 2008; Zweifel et al., 2010), we preferred to correlate the annual TRWi with the NDVI summarized at different time scales (for NDVI time scales, we referred to the average NDVI over the previous n biweekly periods). This is simply because linking TRWi with semi-monthly NDVI can give less reliable results (see Vicente-Serrano et al., 2016). In contrast, the use of the cumulative past NDVI conditions (referring to NDVI time scales), usually provides better

187 relationship with tree-ring growth, as observed in different studies (Arzac et al., 2016; Pasho et al.,
188 2011; Vicente-Serrano et al., 2014).

189 For NDVI time scales, we referred to average NDVI over the previous *n* semi-monthly
190 periods (i.e., two per month). We then correlated the TRWi series with the 24 NDVI semi-monthly
191 series at time scales varying from 1 to 24 semi-monthly periods (i.e., two years). Considering the
192 NDVI values for the previous year allows to account for any possible lag effect, given the possible
193 impact of tree activity and climate conditions during the previous year (Fritts, 1976). For each site
194 chronology (mean TRWi series), we obtained 2304 correlations (48 semi-monthly periods × 48
195 time-scales). This procedure allowed for determining the period with strongest correlation in the
196 two years.

197 The patterns of correlations between the TRWi and the NDVI series was summarized using
198 a S-mode Principal Component Analysis (PCA; (Richman, 1986)). A correlation matrix was used to
199 calculate the Principal Components (PC), and the components were obtained from the original
200 correlation coefficient values using the weight coefficients of each forest in each component. The
201 number of retained components was defined based on the percentage of the total explained variance
202 following the results of the scree-plot. We also mapped the PC loadings to identify represented
203 forests by each component using the available semi-monthly temporal resolution available in the
204 NDVI series, of course including the different cumulative NDVI time scales, from 1 to 24 semi-
205 monthly periods. Finally, each forest was classified by means of a maximum loading rule.

206

207 *2.3.2. Factors explaining the spatial differences in the NDVI-TRWi correlations*

208 Different sources of information were used to determine the influence of biophysical and climate
209 variables on the relationships between the TRWi chronologies and the different NDVI time-scales.
210 First, we assessed the tree species dominating the forest based on the basal area, and their
211 corresponding average NDVI values. Second, we focused on climatic variables [e.g. annual

212 precipitation and mean air temperature and the water balance, defined as the difference between
213 precipitation and reference evapotranspiration (ETo)]. The ETo was calculated following the FAO-
214 56 Penman-Monteith equation (Allen et al., 1998). The climate data were provided at a grid interval
215 similar to that of the NDVI using a newly developed weekly gridded dataset for Spain. This dataset
216 was created using a universal kriging algorithm using elevation as auxiliary variable. Details of the
217 meteorological data processing and the specific gridding and validation methods can be found in
218 Vicente-Serrano et al. (2017).
219 In order to summarize the role of these climatic and environmental conditions and explain the
220 relationship between the TRWi and the NDVI time-scales, the average values for these
221 geographical variables corresponding to each forest were obtained. The contribution of these
222 variables to the spatial differences in the patterns of TRWi response to the NDVI was illustrated by
223 means of different box plots and quantified using a Predictive Discriminant Analysis (PDA) (Hair et
224 al., 1995; Huberty, 1994). PDA allowed assessing which predictors contributed more to the PCs that
225 summarized the TRWi-NDVI dependency. The tree species were included in the PDA as a binary
226 variable, so each tree species was included in the analysis as an individual variable.
227
228 **3. Results**
229 ***3.1. Patterns of relationship between NDVI and TRWi***
230 Figure 2 summarizes the maximum Pearson correlation between NDVI and TRWi, the semi-
231 monthly period at which the maximum correlation is recorded and the NDVI time-scale at which
232 the maximum correlation is recorded. The results are provided for each tree species. In general, the
233 maximum correlations did not show clear differences among tree species, albeit with slightly higher
234 correlations found for *P. halepensis* forests (the species with the highest number of sampled stands;
235 117). Notably, the maximum correlation between NDVI and tree-ring growth is recorded at shorter
236 time-scale (< 10 semi-monthly cumulative periods). Nevertheless, although the magnitude of

correlations and time-scale at which maximum correlation is recorded are quite similar among all species, there are important differences in the semi-monthly period at which maximum correlation was recorded. For instance, in fir species (*Abies alba* and *A. pinsapo*) highest NDVI-TRWi correlations appeared much earlier than those observed for tree species located in drier areas (*P. halepensis*, *P. pinaster*, *P. nigra*, *Juniperus thurifera*, and *Quercus ilex*). Something similar occurred with species predominating in cold and often wet mountainous areas (e.g. *P. sylvestris* and *P. uncinata*) that showed the strongest response earlier than species located in drier areas.

The principal component loadings showed different patterns of correlation between the cumulative NDVI and the annual TRWi (Figure 3). The first Principal Component (PC1) represented the highest percentage of the total explained variance (42.1%), with the maximum correlations between NDVI and TRWi found considering NDVI at time-scales of 10-20 semi-monthly periods at the semi-monthly period 45 (i.e. second half of November). There is a coherent pattern, with NDVI-TRWi correlations that increase in agreement with higher NDVI cumulative periods with the maximum for NDVI values from March to November of the year in which the growth is recorded. The second Principal Component which explained a much lower proportion of the total variance (PC2; 13.1%) also showed a coherent pattern, with the maximum correlation recorded NDVI time scale throughout 15-20 semi-monthly periods, but in the semi-monthly period 26 (second half of January). This means that the cumulative NDVI values between June of the previous year to January of the year of tree-ring formation showed the highest correlation with TRWi. The third Principal Component (PC3; 10.1% of total variance) showed the maximum correlation between NDVI and TRWi around the semi-monthly period 34 (first half of March) considering a cumulative NDVI in a period between November and March. Finally, the remaining Principal Components (PC4-PC6) explained low percentages of the total variance (<7%), suggesting random patterns, which were quite difficult to interpret (Figure 3).

The Figure 4 shows the spatial distribution of the PC loadings corresponding to each PC. PC1 almost showed higher loading values over a high percentage of all forests, summarizing the general pattern of relationships between TRWi and NDVI in the whole Spain. Furthermore, the importance of PC1 is three times higher than the PC2. In comparison to PC1, PC2 showed higher loadings for a lower number of forest, but they were distributed across different regions of Spain. PC3 showed higher loadings for forests located mainly in the Pyrenees (northeastern Spain), whereas PC4 high loadings are distributed along the Pyrenean, besides other forests located in different regions of the country. As opposed to other PCs, both PC5 and PC6 did not reveal clear spatial patterns, with a lower percentage of forests and even very distant forests (PC6).

The patterns of the relationship between NDVI time scales and the TRWi is presented in Figure 5. PC1 showed higher loadings than other components, suggesting that this pattern represents a high percentage of forests in Spain. Nevertheless, higher PC loadings were found for evergreen conifers, mainly living in semi-arid to drought-prone areas (e.g. *P. halepensis*, *P. pinaster*, *P. pinea* and *J. thurifera)*. The pine species dominating in colder and more humid regions (e.g. *P. sylvestris* and *P. uncinata*) showed lower loadings values. Among the oak species, the evergreen *Q. ilex* exhibits the highest loadings. The remaining PCs showed lower loadings, but with some interesting patterns. For example, PC2 showed higher loadings for *C. sativa* and *Q. robur*. Similarly, PC3 indicated higher loadings for *A. alba, P. uncinata* and *F. sylvatica*, which prevail in cool and wet conditions or in moist and temperate regions.

A cluster analysis of forests according to the maximum loading rule showed that PC1 accounts for 304 forests, in comparison to other PCs (e.g. PC5 [69], PC2 [66] and PC4 [64]) (Table 2). Notably, PC1 covered the majority of pine forests, apart from *P. sylvestris* and *P. uncinata*, which are also well-presented in PC3 and PC5. The highest percentage of *A. alba* was recorded in PC3, while *F. sylvatica* shows a higher percentage in PC4.

3.2. Factors explaining the different patterns of NDVI-TRWi couplings

Here we present the comparison between the different PC groups of link between the TRWi and the NDVI time scales and the different environmental characteristics (e.g. air temperature, precipitation, etc.) of the forests included in each PC group. Figure S2 summarizes the average monthly NDVI in the different PC groups. As depicted, there were no clear differences between PC groups during the cold season. Nevertheless, during the warm season, there were significant differences between PC1 and the remaining groups. The average NDVI values of PC1 were lower than those of other PCs during summertime (JJA), indicating that forests represented by this component tended to show lower average NDVI values than other forests. Notably, the highest average NDVI values were recorded for PC3 during summer season.

In addition to lower average NDVI values, the forests represented by PC1 corresponded to climates with higher air temperature (Figures S3 and S4), compared to other PCs. This feature was more pronounced during the warm season. Results also revealed that PC2 showed higher average maximum and minimum air temperatures than PC3 and PC4. These PCs exhibited the lowest averages of air temperature, especially for minimum air temperature. For ETo, PC1 incorporated forests located in dry-warm areas, with higher ETo values than other PCs. This was mostly observed during the warm season, given that ETo is a limiting factor of forest growth in Spain (Figure S5). On the contrary, PC3 and PC4 groups corresponded to forests located in areas characterized by lower ETo values.

Considerable differences in the average precipitation values recorded for the different PC groups were found (Figure S6). PC1 represented not only the forest group characterized by the lowest NDVI values, highest temperatures and ETo, but it was also the group of forests characterized by the lowest average annual precipitation. PC2 was also characterized by low average precipitation values throughout the year. In contrast, PC3 and PC4 were characterized by forests located in areas with higher average precipitation values, even during the dry season.

311 Finally, the water balance, defined as the difference between precipitation and ETo, was
312 summarized for the different forest groups (Figure S7). PC1 and PC2 corresponded to forests
313 characterized by negative water balance, especially from March to September. This suggested that
314 the forests corresponding to PC1 were located mainly in sites with semi-arid climate conditions. On
315 the other hand, PC3 and PC4 showed the higher values for water balance during the warm season.
316 Overall, our findings suggested that TRWi link with NDVI time-scales for the large sample
317 of forests analysed in this study was controlled mainly by the dominant tree species in every forest
318 and the climatic characteristics. This was noticeably confirmed with the Predictive Discriminant
319 Analysis (PDA) that accounts for the relative contribution of each factor to TRWi-NDVI
320 dependency. Table 3 shows the centroids of the groups obtained through a PCA corresponding to
321 the first three functions of the PDA and the percentage of variance explained by each of these
322 functions. The first function showed the highest predictive power, representing 52.8% of the total
323 variance of the PDA. The second and third functions represented 19.7% and 12% of power,
324 respectively. The first function suggested negative values for PC1 and positive values for the
325 remaining components, with the highest values found for PC3. The second function showed its
326 maximum values for PC3 (positive) and PC4 (negative), which means that this function extracted
327 some features of the independent variables that maximize the characteristics of the forests
328 represented by these two components.
329 The structure matrix indicated the correlation of each predictor with the three discriminant
330 functions (Table 4). Function 1 showed negative values for the presence of *P. halepensis* forests in
331 phase with negative values of PC1 in the first function. This suggested that the occurrence of
332 forests characterized by a response between TRWi and the different time-scales of the NDVI was
333 favored in semi-arid (positive values of the climate water balance during the growing season) *P.*
334 *halepensis* forests located in low elevations (given positive value of elevation in PDA1 = 0.43), low
335 average NDVI values during the period of vegetation activity (positive values of the NDVI from

June and October in PDA1), high average temperature and ETo values across the year (negative values of these variables in PDA1) and low precipitation (positive values in PDA1). These conditions were completely the opposite to forests characterized by PC3, which show high positive values for the first PDA function. This indicates that PC3 pattern was more common in mountain cool-wet *A. alba* and *P. uncinata* forests, which show positive values in the first PDA function, located at high elevations, with high average NDVI values during the growing season (June to October) but negative during winter months with snow coverage and low vegetation activity. In addition, the climate characteristics of PC3 pattern were markedly different from those of PC1, given that this pattern was mainly identified in forests characterized by low temperatures and ETo and general humid conditions.

The second PDA function had lower predictive capacity, but with positive values for PC3 and negative values for PC4. A negative value for this second function is obtained for *F. sylvatica* forests, indicating that PC4 pattern was dominant in forest of this species. This pattern was mainly characterized by low temperatures and ETo and high precipitation and climate water balance. In the same context, PC2 was better discriminated by the third PDA function, with a value of 0.53. This PC did not show a clear connection with any forest type, albeit with the positive values found for temperate *Q. robur* forests across wet areas. This pattern was favored by positive average NDVI values during the warm season and positive values of precipitation during the cold season.

4. Discussion and conclusions

This is the first time that the relationship between the interannual variability of the tree-ring growth (TRWi) and the GPP has been established for a variety of forest types under different environmental conditions across Spain. The innovation of this work is mainly related to the high spatial resolution (1.21 km^2) of all input data (e.g. NDVI, climatic data) used for this analysis. This detailed spatial information is extremely important to account for the local-scale environmental

signals influencing the growth of these tree species and to reduce the noise associated to other vegetation types. The high resolution of the spatial data used is also enhanced by a high temporal (semi-monthly) resolution of the NDVI dataset, combined with a dense tree-ring network across different forest ecosystems in Spain (see Gazol et al., 2018).

The obtained results are also important to confidently compare GPP and secondary growth in complex and heterogeneous landscapes, which is a typical feature of the Mediterranean region. Although numerous studies have already compared the NDVI with tree-ring growth over homogeneous forest types, particularly in high-latitude regions (e.g. Lopatin et al., 2006); Kaufmann et al., 2008; Kaufmann et al., 2004), these studies employed coarse resolutions data (64 km^2), mainly the GIMMS dataset. This dataset has frequently been employed to assess the relationships between vegetation activity and tree-ring growth in complex landscapes (e.g. Coulthard et al., 2017; Vicente-Serrano et al., 2016). However, there remains a degree of uncertainty in results obtained based on the GIMMS dataset, particularly at the regional scale. This uncertainty originates mainly from the very low spatial resolution of this product, where multiple cover types can predominate within an individual pixel. Here we accounted for this kind of uncertainty by considering a high-resolution NDVI dataset.

Overall, our findings suggested a positive and significant relationship between the interannual variability in NDVI and the secondary growth measured by means of tree-ring growth series (TRWi). We found similar average correlations among all different forest types. Although this finding seems coherent with what has been evidenced using data of lower spatial resolutions (e.g. Berner et al., 2013; Kaufmann et al., 2008; Vicente-Serrano et al., 2016), our results based on high spatial resolution and long-term coverage of the NDVI data confer more reliability to these results. We noted that the magnitude of the maximum correlation between the TRWi and the semi-monthly NDVI series was quite similar between the semi-arid *P. halepensis* lowland forests and the wet-cool *A. alba* mountain forests. Similar maximum correlations were also found for other tree

386 species from xeric and mesic sites (Coulthard et al., 2017). This suggested that, irrespective of
387 forest type and tree species, secondary growth is favored by a high GPP, leading to higher carbon
388 sinks. There are few experimental studies that have tackled this issue by comparing the relationship
389 between GPP and secondary growth in forest ecosystems, and in general they showed agreement
390 between both variables (Babst et al., 2014a; Poulter et al., 2013) both in cold and humid forests
391 (Krause et al., 2012, Kraus et al., 2016) and in warm and xeric areas (Tognetti et al., 2007).

392 This study demonstrates that the maximum correlations found between NDVI and tree-ring
393 growth were recorded considering cumulative NDVI values, in some cases covering long time
394 periods (6-10 months). This suggests that tree growth is strongly related with GPP at annual scales,
395 since wood production would be related to the accumulation of the carbohydrates synthesized
396 during long periods (Cuny et al., 2015). Secondary growth would be a metric of long-lasting
397 cumulative production (Gough et al., 2008), as carbon must first be used for primary growth in
398 order to form shoots, buds, leaves and fine roots (Stoy et al., 2009). Moreover, temporal lags may
399 be expected due to particular physiological processes. One example can be found during
400 xylogenesis, where there is a delay from the development to the lignification of cells that form the
401 wood (Cuny et al., 2015). Over Spain, the observed patterns stress that the highest positive and
402 significant correlations between NDVI and TRWi across the different analyzed forests are obtained
403 for long time spans of NDVI accumulation.

404 Albeit this general positive and significant correlation of TRWi with cumulative NDVI
405 values, we found that the magnitude of this relationship strongly varies between forest types and
406 environmental conditions (Gazol et al., 2018). There are some dominant patterns of cumulative
407 NDVI-TRWi correlations in the different forest types of Spain. These patterns were very coherent
408 in the shape of this relationship, but also in the characteristics of the tree species involved. As
409 regards the dominant pattern, it is characterized by the highest correlation recorded with a 10-month
410 cumulative NDVI period in November of the year in which the tree-ring is formed. This robust

411 signal was mainly recorded in evergreen tree species located in the semiarid and sub-humid regions
412 of Spain. It represented conifers, such as *P. halepensis*, *P. pinaster*, *P. nigra*, *P. pinea* and *J.*
413 *thurifera,* but also the evergreen oak *Q. ilex,* which was able to inhabit drought-prone areas. These
414 species were characteristics of semi-arid to dry Mediterranean climates. Although they record low
415 average precipitation and climate water balance values, these species show a very good
416 acclimatization to these dry conditions. Even during the strong summer dryness that characterizes
417 their area of distribution, these species are relatively drought tolerant (Zavala et al., 2000), while the
418 GPP during these long periods would affect the annual tree-ring growth (Camarero et al., 2010).
419 The significant contribution of summer season to explaining forest growth was also recorded in oak
420 species from dry Mediterranean and sub-Mediterranean areas (*Q. faginea* and *Q. pyrenaica*), also
421 represented by this pattern of response. Irrespective of summer dryness occurrence, these species
422 form part of the annual tree-ring and carry out other growth processes (e.g. bud and acorn
423 development) in summer (Montserrat-Martí et al., 2009).

424 Other patterns of the NDVI-TRWi relationship represented fewer areas and specific tree
425 species, but with well-defined seasonal patterns. The second pattern summarizing the NDVI-TRWi
426 relationship was characterized by the highest correlation considering the NDVI between June of the
427 previous year and January of the current year. This pattern was much less representative than the
428 first one, with no clear representation of any forest type. The only exception corresponded to *C.*
429 *sativa* forests, which were characterized by higher average NDVI values, lower temperatures and
430 moister conditions than those drawn in the first pattern, representative of broadleaf hardwood
431 species (Babst et al., 2014a; Kagawa et al., 2005; Richardson et al., 2013; Skomarkova et al., 2006).
432 Different studies revealed that the vegetation activity and the NPP over the previous growing season
433 may be important for explaining the forest growth during the following growth season. For
434 example, Babst et al. (2014a) and Babst et al. (2014b) suggest that carbon sequestered after
435 June/July in temperate forests can be used to thicken the cell-walls and/or to be stored in

436 nonstructural carbohydrate reserves, which would contribute tree-ring growth during the next spring
437 (Skomarkova et al., 2006). This process implies a lagged use of synthesized carbohydrates in wood
438 formation, explaining why the primary production of deciduous trees would affect the secondary
439 growth during the following growing season (Kagawa et al., 2005; Richardson et al., 2013).

440 The third pattern of the NDVI-TRWi relationship showed forests related to the cumulative
441 NDVI during the winter and spring season of the current year. This kind of response is mostly
442 represented by the *A. alba* forests located in the Pyrenees, where lower temperatures and higher
443 precipitation values were recorded. The fourth pattern was also mostly characterized by the
444 Pyrenean forests of *A. alba* and *F. sylvatica*, albeit with a positive influence of the summer NDVI
445 on TRWi and an influence of the NDVI recorded during the first part of the previous year. These
446 patterns of response are questionable, given that most active vegetative period of these tree species
447 dominating in cold sites is recorded in late spring and summer (Macias et al., 2006). Nevertheless,
448 several studies have also suggested that the conditions during the prior summer, autumn and winter
449 periods can be relevant to explaining tree-ring growth of these species in Spain (e.g. Hayles et al.,
450 2007; Rozas et al., 2015; Sánchez-Salguero et al., 2013). Kraus et al. (2016) analyzed leaf and
451 xylem phenology at different elevation ranges in Norway spruce forests of the Alps, demonstrating
452 that the length of the xylem cell growth period did not show significant differences, as a function of
453 either elevation or colder conditions, which seemed to lead a longer period of cell maturation in
454 spruce. Furthermore, the Pyrenean silver fir forest growth was sensitive to cold conditions in late
455 winter (February) as well as to dry-warm conditions in the previous early autumn (September). As
456 such, both prior cold and dry conditions can negatively affect subsequent tree-ring formation, NDVI
457 and the NPP in this species (Vicente-Serrano et al., 2015).

458 It seems that phenology of the different tree species contributes significantly to the different
459 patterns of relationship between NDVI and tree-ring growth (e.g. Boulouf Lugo et al., 2012; Čufar
460 et al., 2008). The main patterns of response found in this study are characteristics of

species/regions, with very different tree life cycles driven by temperature. In general, in the forests located in cold areas the tree-ring growth responds to the cumulative NDVI over shorter periods than in the coniferous forests located in more temperate and arid areas. This feature has been identified by Vicente-Serrano et al. (2016) at the global scale, especially in the Alps and the high latitudes of North America, in which cold temperatures and low solar radiation limit the periods of vegetation activity and the duration of tree-ring formation to the boreal summer (Vaganov et al., 1999; Kaufmann et al., 2004; Bergeron et al., 2007). Nevertheless, we must also stress that although there is a clear positive signal between NDVI and TRWi, the magnitude of the correlations usually does not exceed 0.5 in the majority of cases. This finding indicates that GPP and tree-ring growth can be decoupled in a number of years. Also, it suggests that the drivers of vegetation activity can differ as well as the response of the primary production and secondary growth types to some stress factors. There are very few studies that have analyzed the different response of the GPP and secondary growth to climate variability with respect to climate stressors, and even their results are quite contradictory. Recently, Gazol et al. (2018) analyzed the response of the NDVI and the tree-ring growth to the four outstanding droughts, which affected Spain since the 1980s. They found that tree-ring growth is more correlated with drought severity than NDVI. Newberry (2010) analyzed the effects of climate on carbon isotope discrimination ($\delta^{13}C$) in leaves and wood of *Pinus edulis* forests in North America, concluding that that $\delta^{13}C$-climate relationship was stronger for leaf than for tree-ring cellulose, especially at the xeric sites. Del Castillo et al. (2015) and Pasho and Alla (2015) showed contradictory for the Aleppo pine forests in northeastern Spain and Albania, respectively. Overall, these results stressed that the magnitude of the correlations between the NDVI and the tree-ring growth was quite similar across different forest types. Nonetheless, we noted a very high spatial and temporal diversity in the responses of forest secondary growth to NDVI time scales in Spain, with clear distinction between tree species and environmental conditions. As such, our results can contribute not only to determine sensitive periods in vegetation

activity affecting forest growth, but also to assess the possible sensitivity of the GPP and secondary growth to climate change processes.

In summary, in this study we related a satellite-derived measure of vegetation greenness (NDVI), which is driven by canopy formation and leaf-level photosynthesis, with a retrospective reconstruction of secondary growth (interannual variation in tree-ring width). Although we are still in the first methodological stages to reach a prediction of the secondary growth by means of remote sensing imagery, this study has identified the periods, species and bioclimatic conditions in which this is more feasible. This can be useful to advance in a better forest management (both in commercial and protected forest areas), opening the possibility of using remote sensing information to monitor tree growth and forest productivity over large areas. The common lagged response between the vegetation activity (quantified by means of the NDVI) and secondary growth may be also useful to determine in advance possible problems in forest development including dieback. Finally, there is another practical application of our results in order to deep in the knowledge of the sensitivity of forests to climate extreme events and to improve forest adaptation to climate change. Thus, the effects of climate events on the leaf activity may translate in a different way to the secondary growth, being possible to separate between effects. in fact, recent studies have suggested that the response of forests to drought severity is recorded in more depth in the secondary growth (Gazol et al., 2018; Kannenberg et al., 2019; Peña-Gallardo et al., 2018). In this aspect, the results presented here open the door to further studies considering whether drought impacts and legacies in primary and secondary growth are decoupled, and at which spatial and temporal scales. Moreover, the intraannual variation of NDVI will allow better understanding how climate extreme events such as droughts and frosts influence canopy and wood formation, and carbon uptake by forests.

Acknowledgement

This work was supported by the research projects CGL2014-52135-C03-01, CGL2015-69186-C2-1-R, CGL2015-69985-R, CGL2013-48843-C2-1-R, AGL2014-53822-C2-1-R, (BFU2010-21451), PCIN-2015-220, CGL2016-81706-REDT and CGL2017-82216-R financed by the Spanish Commission of Science and Technology and FEDER, 1560/2015: *Herramientas de monitorización de la vegetación mediante modelización ecohidrológica en parques continentales* financed by the *Red de Parques Nacionales*, IMDROFLOOD financed by the Water Works 2014 co-funded call of the European Commission, CROSSDRO financed by the AXIS (Assessment of Cross(X) - sectorial climate Impacts and pathways for Sustainable transformation) JPI-Climate co-funded call of the European Commission and INDECIS, which is part of ERA4CS, an ERA-NET initiated by JPI Climate, and funded by FORMAS (SE), DLR (DE), BMWFW (AT), IFD (DK), MINECO (ES), ANR (FR) with co-funding by the European Union (Grant 690462). financed by the Spanish Commission of Science and Technology and FEDER, and INDECIS, which is part of ERA4CS, an ERA-NET initiated by JPI Climate, and funded by FORMAS (SE), DLR (DE), BMWFW (AT), IFD (DK), MINECO (ES), ANR (FR) with co-funding by the European Union (Grant 690462). Natalia Martin-Hernandez was supported by a doctoral grant by the Aragon Regional Government, Marina Peña-Gallardo was granted by the Spanish Ministry of Economy and Competitiveness and Miquel Tomas-Burguera was supported by a doctoral grant by the Spanish Ministry of Education, Culture and Sport. Raúl Sánchez-Salguero, Antonio Gazol and Gabriel Sangüesa-Barreda were supported by Postdoctoral grants (IJCI-2015-25845, MINECO-FPDI 2013-16600 and FJCI 2016-30121, respectively; FEDER funds). This work also benefited from funding from Xunta de Galicia (PGIDIT06PXIB502262PR, GRC GI-1809, ROCLIGAL-10MDS291009PR), INIA (RTA2006-00117), and Interreg V-A POCTEFA (CANOPEE, 2014-2020-FEDER funds) projects.

References

Alla, A.Q., Pasho, E., Marku, V., 2017. Growth variability and contrasting climatic responses of two Quercus macrolepis stands from Southern Albania. Trees - Struct. Funct. 31, 1491–1504. https://doi.org/10.1007/s00468-017-1564-0

Allen, R.G., Pereira, L.S., Raes, D., Smith, M., 1998. No Title. Crop Evapotranspiration Guidel. Comput. Crop Water Requir.

Arzac, A., García-Cervigón, A.I., Vicente-Serrano, S.M., Loidi, J., Olano, J.M., 2016. Phenological shifts in climatic response of secondary growth allow Juniperus sabina L. to cope with altitudinal and temporal climate variability. Agric. For. Meteorol. 217. https://doi.org/10.1016/j.agrformet.2015.11.011

Babst, F., Bouriaud, O., Alexander, R., Trouet, V., Frank, D., 2014a. Toward consistent measurements of carbon accumulation: A multi-site assessment of biomass and basal area increment across Europe. Dendrochronologia 32, 153–161. https://doi.org/10.1016/j.dendro.2014.01.002

Babst, F., Bouriaud, O., Papale, D., Gielen, B., Janssens, I.A., Nikinmaa, E., Ibrom, A., Wu, J., Bernhofer, C., Köstner, B., Grünwald, T., Seufert, G., Ciais, P., Frank, D., 2014b. Above-ground woody carbon sequestration measured from tree rings is coherent with net ecosystem productivity at five eddy-covariance sites. New Phytol. 201, 1289–1303. https://doi.org/10.1111/nph.12589

Barber, V.A., Juday, G.P., Finney, B.P., 2000. Reduced growth of Alaskan white spruce in the twentieth century from temperature-induced drought stress. Nature 405, 668–673. https://doi.org/10.1038/35015049

Baret, F., Guyot, G., 1991. Potentials and limits of vegetation indices for LAI and APAR assessment. Remote Sens. Environ. 35, 161–173. https://doi.org/10.1016/0034-4257(91)90009-U

560 Bergeron, O., Margolis, H.A., Black, T.A., Coursolle, C., Dunn, A.L., Barr, A.G., Wofsy, S.C.,
561 2007. Comparison of carbon dioxide fluxes over three boreal black spruce forests in Canada.
562 Glob. Chang. Biol. 13, 89–107. https://doi.org/10.1111/j.1365-2486.2006.01281.x
563 Berner, L.T., Beck, P.S.A., Bunn, A.G., Goetz, S.J., 2013. Plant response to climate change along
564 the forest-tundra ecotone in northeastern Siberia. Glob. Chang. Biol. 19, 3449–3462.
565 https://doi.org/10.1111/gcb.12304
566 Bhuyan, U., Zang, C., Vicente-Serrano, S.M., Menzel, A., 2017. Exploring relationships among
567 tree-ring growth, climate variability, and seasonal leaf activity on varying timescales and
568 spatial resolutions. Remote Sens. 9. https://doi.org/10.3390/rs9060526
569 Boulouf Lugo, J., Deslauriers, A., Rossi, S., 2012. Duration of xylogenesis in black spruce
570 lengthened between 1950 and 2010. Ann. Bot. 110, 1099–1108.
571 https://doi.org/10.1093/aob/mcs175
572 Camarero, J.J., Gazol, A., Sangüesa-Barreda, G., Oliva, J., Vicente-Serrano, S.M., 2015. To die or
573 not to die: Early warnings of tree dieback in response to a severe drought. J. Ecol. 103.
574 https://doi.org/10.1111/1365-2745.12295
575 Camarero, J.J., Olano, J.M., Parras, A., 2010. Plastic bimodal xylogenesis in conifers from
576 continental Mediterranean climates. New Phytol. 185, 471–480. https://doi.org/10.1111/j.1469-
577 8137.2009.03073.x
578 Carlson, T.N., Ripley, D.A., 1997. On the relation between NDVI, fractional vegetation cover, and
579 leaf area index. Remote Sens. Environ. 62, 241–252. https://doi.org/10.1016/S0034-
580 4257(97)00104-1
581 Ciais, P., Reichstein, M., Viovy, N., Granier, A., Ogée, J., Allard, V., Aubinet, M., Buchmann, N.,
582 Bernhofer, C., Carrara, A., Chevallier, F., De Noblet, N., Friend, A.D., Friedlingstein, P.,
583 Grünwald, T., Heinesch, B., Keronen, P., Knohl, A., Krinner, G., Loustau, D., Manca, G.,
584 Matteucci, G., Miglietta, F., Ourcival, J.M., Papale, D., Pilegaard, K., Rambal, S., Seufert, G.,

585 Soussana, J.F., Sanz, M.J., Schulze, E.D., Vesala, T., Valentini, R., 2005. Europe-wide
586 reduction in primary productivity caused by the heat and drought in 2003. Nature 437, 529–
587 533. https://doi.org/10.1038/nature03972
588 Cihlar, J., St.-Laurent, L., Dyer, J.A., 1991. Relation between the normalized difference vegetation
589 index and ecological variables. Remote Sens. Environ. 35, 279–298.
590 https://doi.org/10.1016/0034-4257(91)90018-2
591 Coulthard, B.L., Touchan, R., Anchukaitis, K.J., Meko, D.M., Sivrikaya, F., 2017. Tree growth and
592 vegetation activity at the ecosystem-scale in the eastern Mediterranean. Environ. Res. Lett. 12.
593 https://doi.org/10.1088/1748-9326/aa7b26
594 Čufar, K., Prislan, P., De Luis, M., Gričar, J., 2008. Tree-ring variation, wood formation and
595 phenology of beech (Fagus sylvatica) from a representative site in Slovenia, SE Central
596 Europe. Trees - Struct. Funct. 22, 749–758. https://doi.org/10.1007/s00468-008-0235-6
597 Cuny, H.E., Rathgeber, C.B.K., Frank, D., Fonti, P., Makinen, H., Prislan, P., Rossi, S., Del
598 Castillo, E.M., Campelo, F., Vavrčík, H., Camarero, J.J., Bryukhanova, M.V., Jyske, T.,
599 Gricar, J., Gryc, V., De Luis, M., Vieira, J., Cufar, K., Kirdyanov, A.V., Oberhuber, W.,
600 Treml, V., Huang, J.-G., Li, X., Swidrak, I., Deslauriers, A., Liang, E., Nojd, P., Gruber, A.,
601 Nabais, C., Morin, H., Krause, C., King, G., Fournier, M., 2015. Woody biomass production
602 lags stem-girth increase by over one month in coniferous forests. Nat. Plants 1, 1–6.
603 https://doi.org/10.1038/nplants.2015.160
604 del Castillo, J., Voltas, J., Ferrio, J.P., 2015. Carbon isotope discrimination, radial growth, and
605 NDVI share spatiotemporal responses to precipitation in Aleppo pine. Trees - Struct. Funct.
606 29, 223–233. https://doi.org/10.1007/s00468-014-1106-y
607 Donohue, R.J., Roderick, M.L., McVicar, T.R., Farquhar, G.D., 2013. Impact of CO<inf>2</inf>
608 fertilization on maximum foliage cover across the globe's warm, arid environments. Geophys.
609 Res. Lett. 40, 3031–3035. https://doi.org/10.1002/grl.50563

610 Fritts, H.C., 1976. No Title. Tree Rings Clim.
611 Gazol, A., Camarero, J.J., Vicente-Serrano, S.M., Sánchez-Salguero, R., Gutiérrez, E., de Luis, M.,
612 Sangüesa-Barreda, G., Novak, K., Rozas, V., Tíscar, P.A., Linares, J.C., Martín-Hernández,
613 N., Martínez del Castillo, E., Ribas, M., García-González, I., Silla, F., Camisón, A., Génova,
614 M., Olano, J.M., Longares, L.A., Hevia, A., Tomás-Burguera, M., Galván, J.D., 2018. Forest
615 resilience to drought varies across biomes. Glob. Chang. Biol. 24.
616 https://doi.org/10.1111/gcb.14082
617 Gough, C.M., Vogel, C.S., Schmid, H.P., Su, H.-B., Curtis, P.S., 2008. Multi-year convergence of
618 biometric and meteorological estimates of forest carbon storage. Agric. For. Meteorol. 148,
619 158–170. https://doi.org/10.1016/j.agrformet.2007.08.004
620 Granier, A., Reichstein, M., Bréda, N., Janssens, I.A., Falge, E., Ciais, P., Grünwald, T., Aubinet,
621 M., Berbigier, P., Bernhofer, C., Buchmann, N., Facini, O., Grassi, G., Heinesch, B.,
622 Ilvesniemi, H., Keronen, P., Knohl, A., Köstner, B., Lagergren, F., Lindroth, A., Longdoz, B.,
623 Loustau, D., Mateus, J., Montagnani, L., Nys, C., Moors, E., Papale, D., Peiffer, M., Pilegaard,
624 K., Pita, G., Pumpanen, J., Rambal, S., Rebmann, C., Rodrigues, A., Seufert, G., Tenhunen, J.,
625 Vesala, T., Wang, Q., 2007. Evidence for soil water control on carbon and water dynamics in
626 European forests during the extremely dry year: 2003. Agric. For. Meteorol. 143, 123–145.
627 https://doi.org/10.1016/j.agrformet.2006.12.004
628 Grissino-Mayer, H.D., Fritts, H.C., 1997. The International Tree-Ring Data Bank: An enhanced
629 global database serving the global scientific community. Holocene 7, 235–238.
630 https://doi.org/10.1177/095968369700700212
631 Gutman, G.G., 1991. Vegetation indices from AVHRR: An update and future prospects. Remote
632 Sens. Environ. 35, 121–136. https://doi.org/10.1016/0034-4257(91)90005-Q
633 Hair, J.F., Anderson, R.E., Tatham, R.L., Black, W.C., 1995. No Title. Multivar. Data Anal.
634 Hayles, L.A., Gutiérrez, E., Macias, M., Ribas, M., Bosch, O., Camarero, J.J., 2007. Climate

635 increases regional tree-growth variability in Iberian pine forests. Glob. Chang. Biol. 13, 804–
636 815. https://doi.org/10.1111/j.1365-2486.2007.01322.x
637 Herrmann, S.M., Anyamba, A., Tucker, C.J., 2005. Recent trends in vegetation dynamics in the
638 African Sahel and their relationship to climate. Glob. Environ. Chang. 15, 394–404.
639 https://doi.org/10.1016/j.gloenvcha.2005.08.004
640 Holmes, R.L., 1983. Computer-assisted quality control in tree-ring dating and measurement. Tree-
641 Ring Bull. 44, 69–75.
642 Huberty, C.J., 1994. No Title. Appl. Discrim. Anal.
643 Kagawa, A., Sugimoto, A., Yamashita, K., Abe, H., 2005. Temporal photosynthetic carbon isotope
644 signatures revealed in a tree ring through ^{13}CO<inf>2</inf> pulse-labelling. Plant, Cell
645 Environ. 28, 906–915. https://doi.org/10.1111/j.1365-3040.2005.01343.x
646 Kannenberg, S.A., Novick, K.A., Alexander, M.R., Maxwell, J.T., Moore, D.J.P., Phillips, R.P.,
647 Anderegg, W.R.L., 2019. Linking drought legacy effects across scales: From leaves to tree
648 rings to ecosystems. Glob. Chang. Biol. 0. https://doi.org/10.1111/gcb.14710
649 Kaufmann, R.K., D'Arrigo, R.D., Laskowski, C., Myneni, R.B., Zhou, L., Davi, N.K., 2004. The
650 effect of growing season and summer greenness on northern forests. Geophys. Res. Lett. 31.
651 https://doi.org/10.1029/2004GL019608
652 Kaufmann, R.K., D'Arrigo, R.D., Paletta, L.F., Tian, H.Q., Jolly, W.M., Myneni, R.B., 2008.
653 Identifying climatic controls on ring width: The timing of correlations between tree rings and
654 NDVI. Earth Interact. 12, 1–14. https://doi.org/10.1175/2008EI263.1
655 Kogan, F.N., 1997. Global Drought Watch from Space. Bull. Am. Meteorol. Soc. 78, 621–636.
656 https://doi.org/10.1175/1520-0477(1997)078<0621:GDWFS>2.0.CO;2
657 Kraus, C., Zang, C., Menzel, A., 2016. Elevational response in leaf and xylem phenology reveals
658 different prolongation of growing period of common beech and Norway spruce under warming
659 conditions in the Bavarian Alps. Eur. J. For. Res. 135, 1011–1023.

https://doi.org/10.1007/s10342-016-0990-7

Krause, K., Cherubini, P., Bugmann, H., Schleppi, P., 2012. Growth enhancement of Picea abies trees under long-term, low-dose N addition is due to morphological more than to physiological changes. Tree Physiol. 32, 1471–1481. https://doi.org/10.1093/treephys/tps109

Leavitt, S.W., Chase, T.N., Rajagopalan, B., Lee, E., Lawrence, P.J., 2008. Southwestern U.S. tree-ring carbon isotope indices as a possible proxy for reconstruction of greenness of vegetation. Geophys. Res. Lett. 35. https://doi.org/10.1029/2008GL033894

Liang, E., Eckstein, D., Liu, H., 2009. Assessing the recent grassland greening trend in a long-term context based on tree-ring analysis: A case study in North China. Ecol. Indic. 9, 1280–1283. https://doi.org/10.1016/j.ecolind.2009.02.007

Lopatin, E., Kolström, T., Spiecker, H., 2006. Determination of forest growth trends in Komi Republic (northwestern Russia): Combination of tree-ring analysis and remote sensing data. Boreal Environ. Res. 11, 341–353.

Lundqvist, S.-O., Seifert, S., Grahn, T., Olsson, L., García-Gil, M.R., Karlsson, B., Seifert, T., 2018. Age and weather effects on between and within ring variations of number, width and coarseness of tracheids and radial growth of young Norway spruce. Eur. J. For. Res. 137, 719–743. https://doi.org/10.1007/s10342-018-1136-x

Macias, M., Andreu, L., Bosch, O., Camarero, J.J., Gutiérrez, E., 2006. Increasing aridity is enhancing silver fir (Abies alba Mill.) water stress in its south-western distribution limit. Clim. Change 79, 289–313. https://doi.org/10.1007/s10584-006-9071-0

Malmström, C.M., Thompson, M.V., Juday, G.P., Los, S.O., Randerson, J.T., Field, C.B., 1997. Interannual variation in global-scale net primary production: Testing model estimates. Global Biogeochem. Cycles 11, 367–392. https://doi.org/10.1029/97GB01419

Martín-Hernández, N., Vicente-Serrano, S.M., Beguería, S., Azorín-Molina, C., Reig, F., Zabalza, J., 2017. Three decades of NOAA-AVHRR data to assess vegetation dynamics in the Iberian

685 Peninsula and the Balearic Islands: the IBERIAN NDVI dataset, in: Sobrino, J. (Ed.), Fifth
686 Recent Advances in Quantitative Remote Sensing. Universitat de Valencia, Valencia, pp. 168–
687 173.
688 Montserrat-Martí, G., Camarero, J.J., Palacio, S., Pérez-Rontomé, C., Milla, R., Albuixech, J.,
689 Maestro, M., 2009. Summer-drought constrains the phenology and growth of two coexisting
690 Mediterranean oaks with contrasting leaf habit: Implications for their persistence and
691 reproduction. Trees - Struct. Funct. 23, 787–799. https://doi.org/10.1007/s00468-009-0320-5
692 Myneni, R.B., Hall, F.G., Sellers, P.J., Marshak, A.L., 1995. Interpretation of spectral vegetation
693 indexes. IEEE Trans. Geosci. Remote Sens. 33, 481–486. https://doi.org/10.1109/36.377948
694 Nemani, R.R., Keeling, C.D., Hashimoto, H., Jolly, W.M., Piper, S.C., Tucker, C.J., Myneni, R.B.,
695 Running, S.W., 2003. Climate-driven increases in global terrestrial net primary production
696 from 1982 to 1999. Science (80-.). 300, 1560–1563. https://doi.org/10.1126/science.1082750
697 Newberry, T.L., 2010. Effect of climatic variability on $\delta^{13}C$ and tree-ring growth in piñon pine
698 (Pinus edulis). Trees - Struct. Funct. 24, 551–559. https://doi.org/10.1007/s00468-010-0426-9
699 Olson, M.E., Soriano, D., Rosell, J.A., Anfodillo, T., Donoghue, M.J., Edwards, E.J., León-Gómez,
700 C., Dawson, T., Camarero Martínez, J.J., Castorena, M., Echeverría, A., Espinosa, C.I.,
701 Fajardo, A., Gazol, A., Isnard, S., Lima, R.S., Marcati, C.R., Méndez-Alonzo, R., 2018. Plant
702 height and hydraulic vulnerability to drought and cold. Proc. Natl. Acad. Sci. 115, 7551–7556.
703 https://doi.org/10.1073/pnas.1721728115
704 Orwig, D.A., Abrams, M.D., 1997. Variation in radial growth responses to drought among species,
705 site, and canopy strata. Trees - Struct. Funct. 11, 474–484.
706 https://doi.org/10.1007/s004680050110
707 Pasho, E., Alla, A.Q., 2015. Climate impacts on radial growth and vegetation activity of two co-
708 existing Mediterranean pine species. Can. J. For. Res. 45, 1748–1756.
709 https://doi.org/10.1139/cjfr-2015-0146

710 Pasho, E., Camarero, J.J., de Luis, M., Vicente-Serrano, S.M., 2011. Impacts of drought at different
711 time scales on forest growth across a wide climatic gradient in north-eastern Spain. Agric. For.
712 Meteorol. 151. https://doi.org/10.1016/j.agrformet.2011.07.018
713 Peguero-Pina, J.J., Camarero, J.J., Abadía, A., Martín, E., González-Cascón, R., Morales, F., Gil-
714 Pelegrín, E., 2007. Physiological performance of silver-fir (Abies alba Mill.) populations under
715 contrasting climates near the south-western distribution limit of the species. Flora Morphol.
716 Distrib. Funct. Ecol. Plants 202, 226–236. https://doi.org/10.1016/j.flora.2006.06.004
717 Peña-Gallardo, M., Vicente-Serrano, S.M., Camarero, J.J., Gazol, A., Sánchez-Salguero, R.,
718 Domínguez-Castro, F., El Kenawy, A., Beguería-Portugés, S., Gutiérrez, E., de Luis, M.,
719 Sangüesa-Barreda, G., Novak, K., Rozas, V., Tíscar, P.A., Linares, J.C., del Castillo, E., Ribas
720 Matamoros, M., García-González, I., Silla, F., Camisón, Á., Génova, M., Olano, J.M.,
721 Longares, L.A., Hevia, A., Galván, J.D., 2018. Drought Sensitiveness on Forest Growth in
722 Peninsular Spain and the Balearic Islands. Forests 9.
723 Pinzon, J.E., Tucker, C.J., 2014. A non-stationary 1981-2012 AVHRR NDVI<inf>3g</inf>time
724 series. Remote Sens. 6, 6929–6960. https://doi.org/10.3390/rs6086929
725 Poulter, B., Pederson, N., Liu, H., Zhu, Z., D'Arrigo, R., Ciais, P., Davi, N., Frank, D., Leland, C.,
726 Myneni, R., Piao, S., Wang, T., 2013. Recent trends in Inner Asian forest dynamics to
727 temperature and precipitation indicate high sensitivity to climate change. Agric. For. Meteorol.
728 178–179, 31–45. https://doi.org/10.1016/j.agrformet.2012.12.006
729 Richardson, A.D., Carbone, M.S., Keenan, T.F., Czimczik, C.I., Hollinger, D.Y., Murakami, P.,
730 Schaberg, P.G., Xu, X., 2013. Seasonal dynamics and age of stemwood nonstructural
731 carbohydrates in temperate forest trees. New Phytol. 197, 850–861.
732 https://doi.org/10.1111/nph.12042
733 Richman, M.B., 1986. Rotation of principal components. J. Climatol. 6, 293–335.
734 https://doi.org/10.1002/joc.3370060305

735 Rötzer, T., Seifert, T., Gayler, S., Priesack, E., Pretzsch, H., 2012. Effects of Stress and Defence
736 Allocation on Tree Growth: Simulation Results at the Individual and Stand Level., in: In:
737 Matyssek R., Schnyder H., Oßwald W., Ernst D., Munch J., Pretzsch H. (Eds) Growth and
738 Defence in Plants. Ecological Studies (Analysis and Synthesis), Vol 220. Springer, Berlin,
739 Heidelberg.
740 Rozas, V., Camarero, J.J., Sangüesa-Barreda, G., Souto, M., García-González, I., 2015. Summer
741 drought and ENSO-related cloudiness distinctly drive Fagus sylvatica growth near the species
742 rear-edge in northern Spain. Agric. For. Meteorol. 201, 153–164.
743 https://doi.org/10.1016/j.agrformet.2014.11.012
744 Rubio-Cuadrado, Á., Camarero, J.J., del Río, M., Sánchez-González, M., Ruiz-Peinado, R., Bravo-
745 Oviedo, A., Gil, L., Montes, F., 2018. Drought modifies tree competitiveness in an oak-beech
746 temperate forest. For. Ecol. Manage. 429, 7–17. https://doi.org/10.1016/j.foreco.2018.06.035
747 Sánchez-Salguero, R., Camarero, J.J., Carrer, M., Gutiérrez, E., Alla, A.Q., Andreu-Hayles, L.,
748 Hevia, A., Koutavas, A., Martínez-Sancho, E., Nola, P., Papadopoulos, A., Pasho, E.,
749 Toromani, E., Carreira, J.A., Linares, J.C., 2017. Climate extremes and predicted warming
750 threaten Mediterranean Holocene firs forests refugia. Proc. Natl. Acad. Sci. U. S. A. 114,
751 E10142–E10150. https://doi.org/10.1073/pnas.1708109114
752 Sánchez-Salguero, R., Camarero, J.J., Dobbertin, M., Fernández-Cancio, T., Vilà-Cabrera, A.,
753 Manzanedo, R.D., Zavala, M.A., Navarro-Cerrillo, R.M., 2013. Contrasting vulnerability and
754 resilience to drought-induced decline of densely planted vs. natural rear-edge Pinus nigra
755 forests. For. Ecol. Manage. 310, 956–967. https://doi.org/10.1016/j.foreco.2013.09.050
756 Skomarkova, M.V., Vaganov, E.A., Mund, M., Knohl, A., Linke, P., Boerner, A., Schulze, E.-D.,
757 2006. Inter-annual and seasonal variability of radial growth, wood density and carbon isotope
758 ratios in tree rings of beech (Fagus sylvatica) growing in Germany and Italy. Trees - Struct.
759 Funct. 20, 571–586. https://doi.org/10.1007/s00468-006-0072-4

760 Stoy, P.C., Richardson, A.D., Baldocchi, D.D., Katul, G.G., Stanovick, J., Mahecha, M.D.,
761 Reichstein, M., Detto, M., Law, B.E., Wohlfahrt, G., Arriga, N., Campos, J., McCaughey, J.H.,
762 Montagnani, L., Paw U, K.T., Sevanto, S., Williams, M., 2009. Biosphere-atmosphere
763 exchange of CO<inf>2</inf>in relation to climate: A cross-biome analysis across multiple
764 time scales. Biogeosciences 6, 2297–2312. https://doi.org/10.5194/bg-6-2297-2009
765 Tognetti, R., Cherubini, P., Marchi, S., Raschi, A., 2007. Leaf traits and tree rings suggest different
766 water-use and carbon assimilation strategies by two co-occurring Quercus species in a
767 Mediterranean mixed-forest stand in Tuscany, Italy. Tree Physiol. 27, 1741–1751.
768 https://doi.org/10.1093/treephys/27.12.1741
769 Tucker, C.J., Pinzon, J.E., Brown, M.E., Slayback, D.A., Pak, E.W., Mahoney, R., Vermote, E.F.,
770 El Saleous, N., 2005. An extended AVHRR 8-km NDVI dataset compatible with MODIS and
771 SPOT vegetation NDVI data. Int. J. Remote Sens. 26, 4485–4498.
772 https://doi.org/10.1080/01431160500168686
773 Tucker, C.J., Vanpraet, C., Boerwinkel, E., Gaston, A., 1983. Satellite remote sensing of total dry
774 matter production in the Senegalese Sahel. Remote Sens. Environ. 13, 461–474.
775 https://doi.org/10.1016/0034-4257(83)90053-6
776 Vaganov, E.A., Hughes, M.K., Kirdyanov, A.V., Schweingruber, F.H., Silkin, P.P., 1999. Influence
777 of snowfall and melt timing on tree growth in subarctic Eurasia. Nature 400, 149–151.
778 https://doi.org/10.1038/22087
779 Vicente-Serrano, S.M., 2007. Evaluating the impact of drought using remote sensing in a
780 Mediterranean, Semi-arid Region. Nat. Hazards 40. https://doi.org/10.1007/s11069-006-0009-
781 7
782 Vicente-Serrano, S.M., Camarero, J.J., Azorin-Molina, C., 2014. Diverse responses of forest growth
783 to drought time-scales in the Northern Hemisphere. Glob. Ecol. Biogeogr. 23.
784 https://doi.org/10.1111/geb.12183

785 Vicente-Serrano, S.M., Camarero, J.J., Olano, J.M., Martín-Hernández, N., Peña-Gallardo, M.,
786 Tomás-Burguera, M., Gazol, A., Azorin-Molina, C., Bhuyan, U., El Kenawy, A., 2016.
787 Diverse relationships between forest growth and the Normalized Difference Vegetation Index
788 at a global scale. Remote Sens. Environ. 187. https://doi.org/10.1016/j.rse.2016.10.001
789 Vicente-Serrano, S.M., Camarero, J.J., Zabalza, J., Sangüesa-Barreda, G., López-Moreno, J.I.,
790 Tague, C.L., 2015. Evapotranspiration deficit controls net primary production and growth of
791 silver fir: Implications for Circum-Mediterranean forests under forecasted warmer and drier
792 conditions. Agric. For. Meteorol. 206. https://doi.org/10.1016/j.agrformet.2015.02.017
793 Vicente-Serrano, S.M., Lasanta, T., Romo, A., 2004. Analysis of spatial and temporal evolution of
794 vegetation cover in the Spanish central pyrenees: Role of human management. Environ.
795 Manage. 34. https://doi.org/10.1007/s00267-003-0022-5
796 Vicente-Serrano, S.M., Tomas-Burguera, M., Beguería, S., Reig, F., Latorre, B., Peña-Gallardo, M.,
797 Luna, M.Y., Morata, A., González-Hidalgo, J.C., 2017. A High Resolution Dataset of Drought
798 Indices for Spain. Data 2.
799 Wylie, B.K., Meyer, D.J., Tieszen, L.L., Mannel, S., 2002. Satellite mapping of surface biophysical
800 parameters at the biome scale over the North American grasslands a case study. Remote Sens.
801 Environ. 79, 266–278. https://doi.org/10.1016/S0034-4257(01)00278-4
802 Zavala, M.A., Espelta, J.M., Retana, J., 2000. Constraints and trade-offs in Mediterranean plant
803 communities: The case of holm oak-Aleppo pine forests. Bot. Rev. 66, 119–149.
804 https://doi.org/10.1007/BF02857785
805 Zhao, M., Running, S.W., 2010. Drought-induced reduction in global terrestrial net primary
806 production from 2000 through 2009. Science (80-.). 329, 940–943.
807 https://doi.org/10.1126/science.1192666
808 Zhou, L., Tucker, C.J., Kaufmann, R.K., Slayback, D., Shabanov, N.V., Myneni, R.B., 2001.
809 Variations in northern vegetation activity inferred from satellite data of vegetation index

during 1981 to 1999. J. Geophys. Res. Atmos. 106, 20069–20083. https://doi.org/10.1029/2000JD000115

Zweifel, R., Eugster, W., Etzold, S., Dobbertin, M., Buchmann, N., Häsler, R., 2010. Link between continuous stem radius changes and net ecosystem productivity of a subalpine Norway spruce forest in the Swiss Alps. New Phytol. 187, 819–830. https://doi.org/10.1111/j.1469-8137.2010.03301.x

823 Table 1: Tree species, abbreviations and number of sampled forests. The annual water balance was defined
824 as the difference between precipitation and the reference evapotranspiration (ETo).

Tree species (code)	Number of forests	Mean NDVI	Mean annual temperature (ºC)	Annual Precipitation sums (mm)	Annual water balance (mm)
Abies alba (ABAL)	48	0.32	13.06	1441.08	486.46
Abies pinsapo (ABPN)	15	0.26	17.64	1469.77	296.28
Castanea sativa (CASA)	10	0.43	17.53	928.83	-139.96
Fagus sylvatica (FASY)	51	0.39	14.72	1213.45	283.87
Juniperus thurifera (JUTH)	16	0.28	17.21	690.61	-397.87
Pinus halepensis (PIHA)	117	0.26	19.99	600.31	-617.18
Pinus nigra (PINI)	66	0.29	17.06	753.91	-344.72
Pinus pinaster (PIPI)	20	0.32	18.78	705.39	-454.55
Pinus pinea (PIPN)	9	0.27	20.10	551.33	-665.18
Pinus sylvestris (PISY)	76	0.32	14.74	959.48	-36.94
Pinus uncinata (PIUN)	39	0.23	10.18	1445.58	576.37
Quercus faginea (QUFA)	19	0.36	16.82	976.20	-125.80
Quercus ilex (QUIL)	5	0.31	17.42	786.00	-338.58
Quercus petraea (QUPE)	7	0.41	15.67	1062.21	114.98
Quercus pyrenaica (QUPY)	34	0.40	16.22	878.32	-142.55
Quercus robur (QURO)	34	0.46	16.22	1484.47	594.25

825

826

Table 2: Percentage of species represented by each PC following the maximum loading rule.

	PC1 (304)	PC2 (66)	PC3 (38)	PC4 (64)	PC5 (69)	PC6 (22)
ABAL	12.5	8.3	35.4	20.8	10.4	12.5
ABPN	53.3	13.3	6.7	0.0	20.0	6.7
CASA	40.0	30.0	0.0	0.0	30.0	0.0
FASY	39.2	17.6	2.0	31.4	3.9	5.9
JUTH	75.0	18.8	0.0	0.0	6.3	0.0
PIHA	83.8	6.0	0.9	0.9	6.0	2.6
PINI	68.2	10.6	4.5	3.0	9.1	4.5
PIPI	90.0	5.0	0.0	0.0	5.0	0.0
PIPN	100.0	0.0	0.0	0.0	0.0	0.0
PISY	42.1	9.2	10.5	13.2	23.7	1.3
PIUN	25.6	12.8	10.3	35.9	12.8	2.6
QUFA	52.6	10.5	0.0	5.3	26.3	5.3
QUIL	100.0	0.0	0.0	0.0	0.0	0.0
QUPE	57.1	28.6	14.3	0.0	0.0	0.0
QUPY	32.4	20.6	2.9	11.8	29.4	0.0
QURO	35.3	20.6	2.9	17.6	8.8	8.8

Table 3: Centroids of the groups obtained through a principal components analysis corresponding to the first three functions of the predictive discriminant analysis (PDA). The variance explained by each PDA is shown in parentheses.

	Function		
Components	PDA 1 (52.8%)	PDA 2 (19.7%)	PDA 3 (12.0%)
1	-0.583	0.039	-0.060
2	0.305	-0.063	0.530
3	1.533	0.792	-0.243
4	0.818	-1.045	-0.057
5	0.568	0.209	-0.406
6	0.479	0.490	1.133

Table 4: Structure matrix of the first three components of the predictive discriminant analysis (PDA). The table shows the correlation values of each predictor variable with the three discriminant functions. The variables most representative in each of the functions are in bold.

Variable type	VARIABLES	FUNCTION 1	FUNCTION 2	FUNCTION 3	Variable type	VARIABLES	FUNCTION 1	FUNCTION 2	FUNCTION 3
Tree species	ABAL	0.254	0.169	-0.049	Monthly mean minimum temperatures	T. MIN. MAY.	**-0.646**	0.33	0.104
	ABPN	-0.065	0.08	0.084		T. MIN. JUN.	**-0.661**	0.33	0.053
	CASA	0.067	-0.005	-0.037		T. MIN. JUL.	**-0.66**	0.33	-0.014
	FASY	0.111	**-0.496**	0.294		T. MIN. AUG.	**-0.659**	0.326	-0.018
	JUTH	-0.121	0.019	-0.018		T. MIN. SEP.	**-0.651**	0.298	0.035
	PIHA	**-0.458**	0.158	-0.081		T. MIN. OCT.	**-0.622**	0.279	0.094
	PINI	-0.048	0.021	-0.162		T. MIN. NOV.	**-0.601**	0.246	0.138
	PIPI	-0.075	-0.033	0.052		T. MIN. DEC.	**-0.582**	0.219	0.156
	PIPN	-0.157	0.028	-0.071	Monthly evapotranspiration	ETo JAN.	**-0.402**	0.11	-0.025
	PISY	0.071	0.025	-0.086		ETo FEB.	**-0.609**	0.253	-0.008
	PIUN	0.27	-0.276	-0.076		ETo MAR.	**-0.681**	0.351	-0.018
	QUFA	-0.022	0.042	-0.045		ETo APRIL	**-0.693**	0.376	-0.008
	QUIL	0.026	0.016	-0.028		ETo MAY.	**-0.66**	0.398	-0.047
	QUPE	0.093	0.068	0.046		ETo JUN.	**-0.595**	0.393	-0.111
	QUPY	0.136	0.152	0.024		ETo JUL.	**-0.518**	0.367	-0.193
	QURO	0.114	0.132	0.29		ETo AUG.	**-0.513**	0.379	-0.152
Topography	ELEVATION	**0.427**	-0.253	-0.239		ETo SEP.	**-0.624**	0.391	-0.067
Monthly NDVI values	NDVI JAN.	-0.16	0.248	0.066		ETo OCT.	**-0.648**	0.349	-0.03
	NDVI FEB.	-0.146	0.275	0.131		ETo NOV.	**-0.5**	0.187	-0.022
	NDVI MAR.	-0.091	0.311	0.147		ETo DEC.	-0.318	0.041	-0.038
	NDVI APR.	-0.012	0.285	0.168	Monthly precipitation	PRECIP JAN.	0.349	-0.006	0.331
	NDVI MAY.	0.253	0.223	0.227		PRECIP FEB.	0.275	0.018	0.331
	NDVI JUN.	**0.513**	0.1	0.275		PRECIP MAR.	0.396	-0.05	0.339

	NDVI JUL.	**0.527**	-0.01	0.205		PRECIP APR.	**0.582**	-0.149	0.252
	NDVI AUG.	**0.694**	0.007	0.329		PRECIP MAY.	**0.684**	-0.264	0.118
	NDVI SEP.	**0.673**	0.028	0.279		PRECIP JUN.	**0.663**	-0.298	0.001
	NDVI OCT.	**0.544**	0.083	0.258		PRECIP JUL.	**0.65**	-0.328	0.024
	NDVI NOV.	0.177	0.187	0.153		PRECIP AUG.	**0.544**	-0.367	-0.033
	NDVI DEC.	-0.093	0.258	0.028		PRECIP SEP.	**0.545**	-0.292	0.059
Monthly mean maximum temperatures	T. MAX. JAN.	**-0.648**	0.313	0.187		PRECIP OCT.	**0.435**	-0.132	0.24
	T. MAX. FEB.	**-0.671**	0.359	0.19		PRECIP NOV.	**0.444**	-0.097	0.315
	T. MAX. MAR.	**-0.674**	0.388	0.17		PRECIP DEC.	0.302	0.001	0.305
	T. MAX. APR.	**-0.677**	0.397	0.141	Monthly climatic water balance	BALANCE JAN.	0.385	-0.02	0.321
	T. MAX. MAY.	**-0.67**	**0.417**	0.098		BALANCE FEB.	0.348	-0.022	0.309
	T. MAX. JUN.	**-0.654**	**0.428**	0.045		BALANCE MAR.	**0.504**	-0.128	0.294
	T. MAX. JUL.	**-0.634**	**0.412**	-0.032		BALANCE APRIL	**0.653**	-0.229	0.192
	T. MAX. AUG.	**-0.638**	**0.418**	-0.004		BALANCE MAY	**0.705**	-0.323	0.098
	T. MAX. SEP.	**-0.666**	**0.406**	0.097		BALANCE JUN.	**0.672**	-0.359	0.051
	T. MAX. OCT.	**-0.68**	0.385	0.154		BALANCE JUL.	**0.631**	-0.374	0.115
	T. MAX. NOV.	**-0.667**	0.335	0.176		BALANCE AUG.	**0.572**	-0.4	0.045
	T. MAX. DEC.	**-0.644**	0.286	0.18		BALANCE SEP.	**0.605**	-0.344	0.066
Monthly mean minimum temperatures	T. MIN. JAN.	**-0.593**	0.232	0.159		BALANCE OCT.	**0.517**	-0.188	0.219
	T. MIN. FEB.	**-0.617**	0.271	0.156		BALANCE NOV.	**0.485**	-0.115	0.303
	T. MIN. MAR.	**-0.62**	0.298	0.139		BALANCE DEC.	0.328	-0.004	0.299
	T. MIN. APR.	**-0.638**	0.328	0.148					

Figures

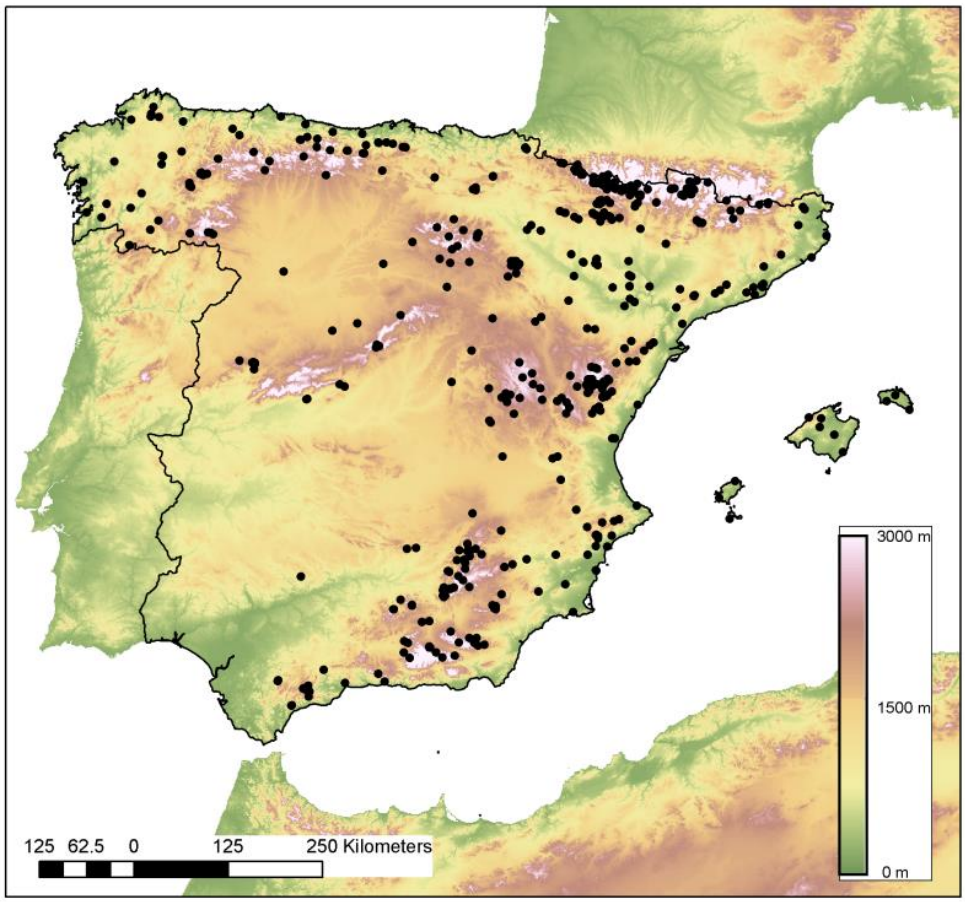

Figure 1: Spatial distribution of the tree-ring dataset available in the Spanish peninsula and the Balearic Islands. Each point represents a sampled forest.

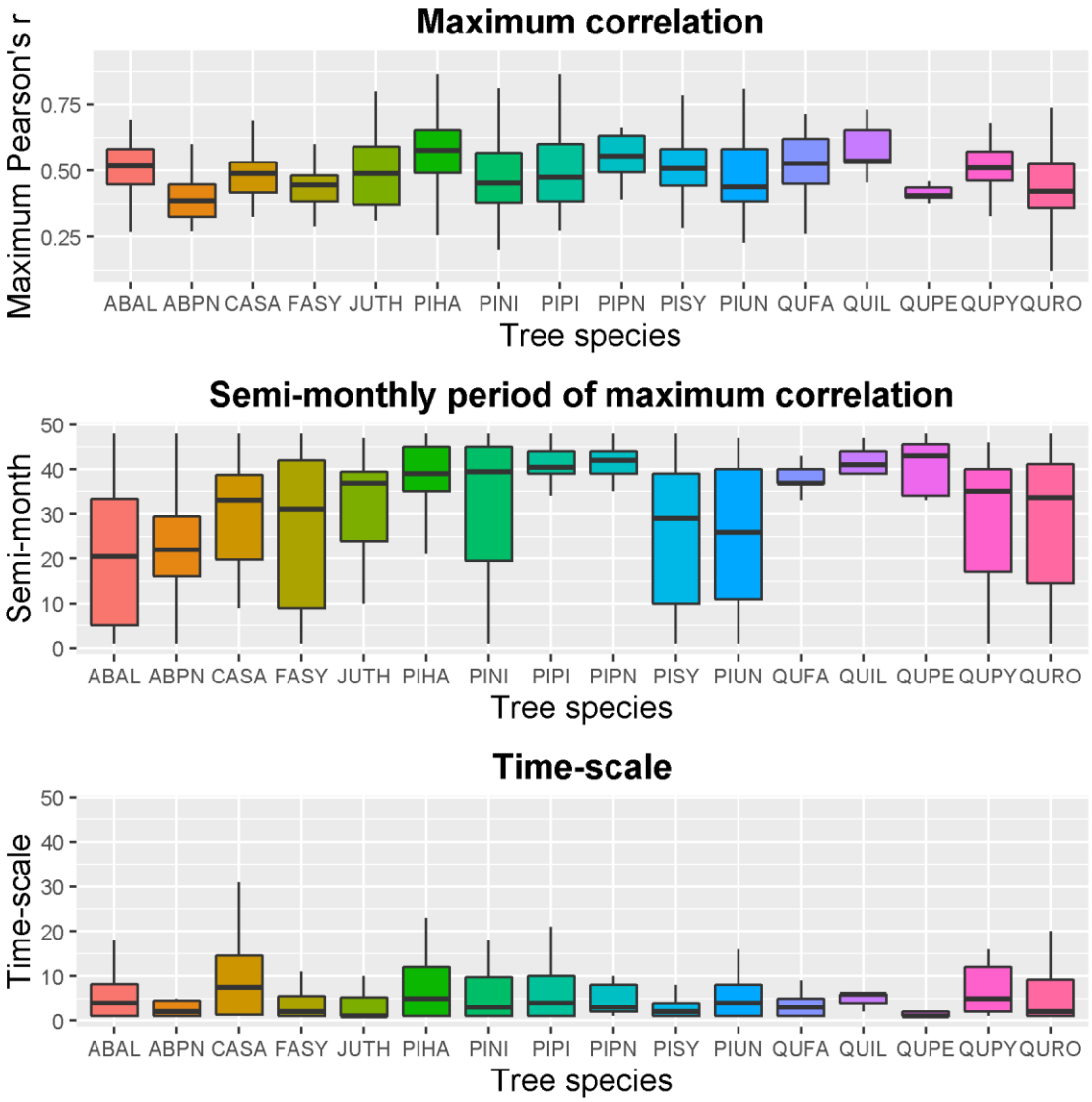

Figure 2. [Upper] Box plots showing the maximum Pearson correlation obtained between the NDVI series at different time scales and the indexed tree-ring width series for each tree species; [central] the semi-monthly period at which the maximum correlation is recorded, and [lower] the NDVI time-scale (in semi-months) at which the maximum correlation is recorded. All codes of species correspond to those listed in Table 1. For each box plot, the central solid line indicates the median. The whiskers represent the 10th and the 90th, while the 25th and the 75th are plotted as the vertical lines of the bounding boxes.

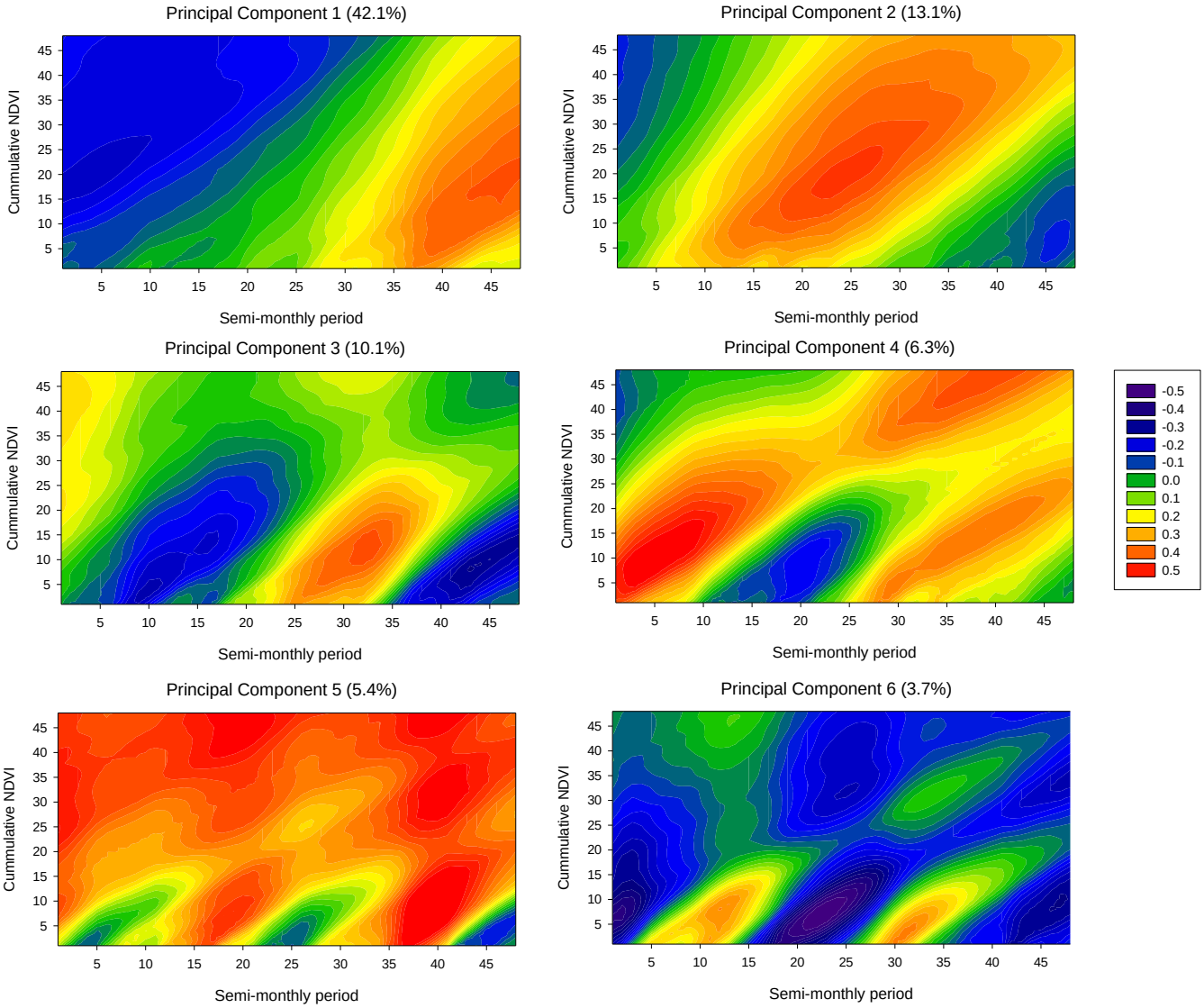

Figure 3. Principal Component loadings extracted representing the main patterns of NDVI-TRWi correlations. The percentage of the variance represented by each component is shown between brackets. The values of the components are represented in the original variable (correlation).

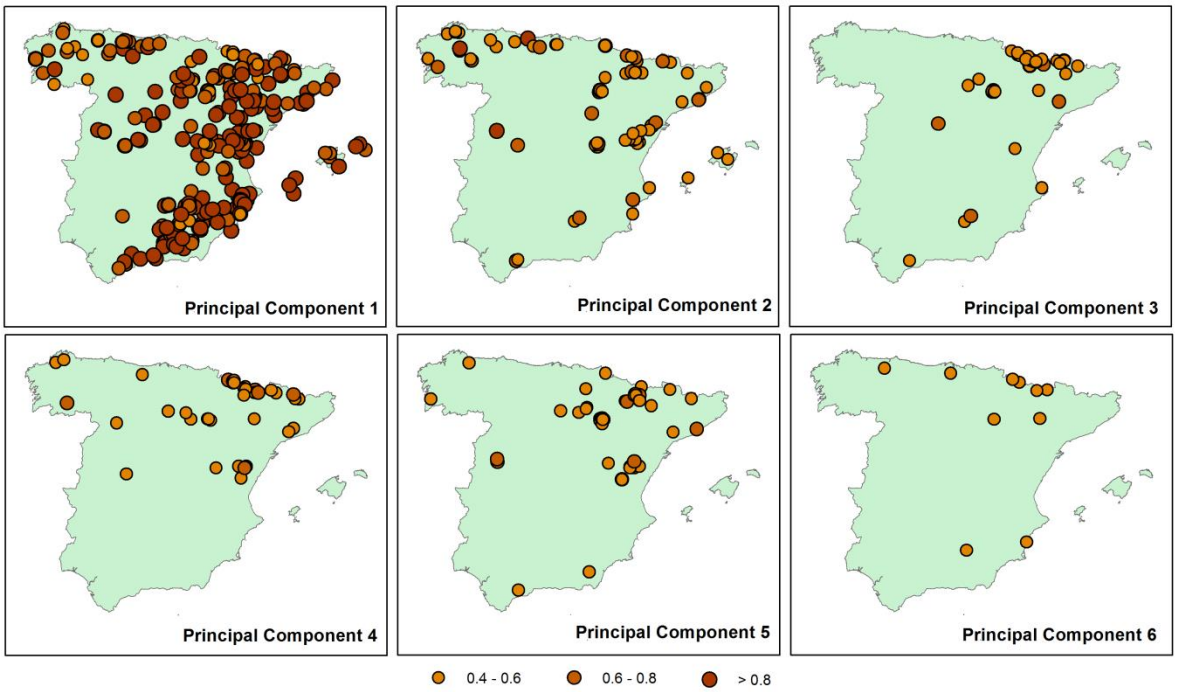

Figure 4. Spatial distribution of the Principal Component loadings for the six principal components extracted. Only significant loadings are shown.

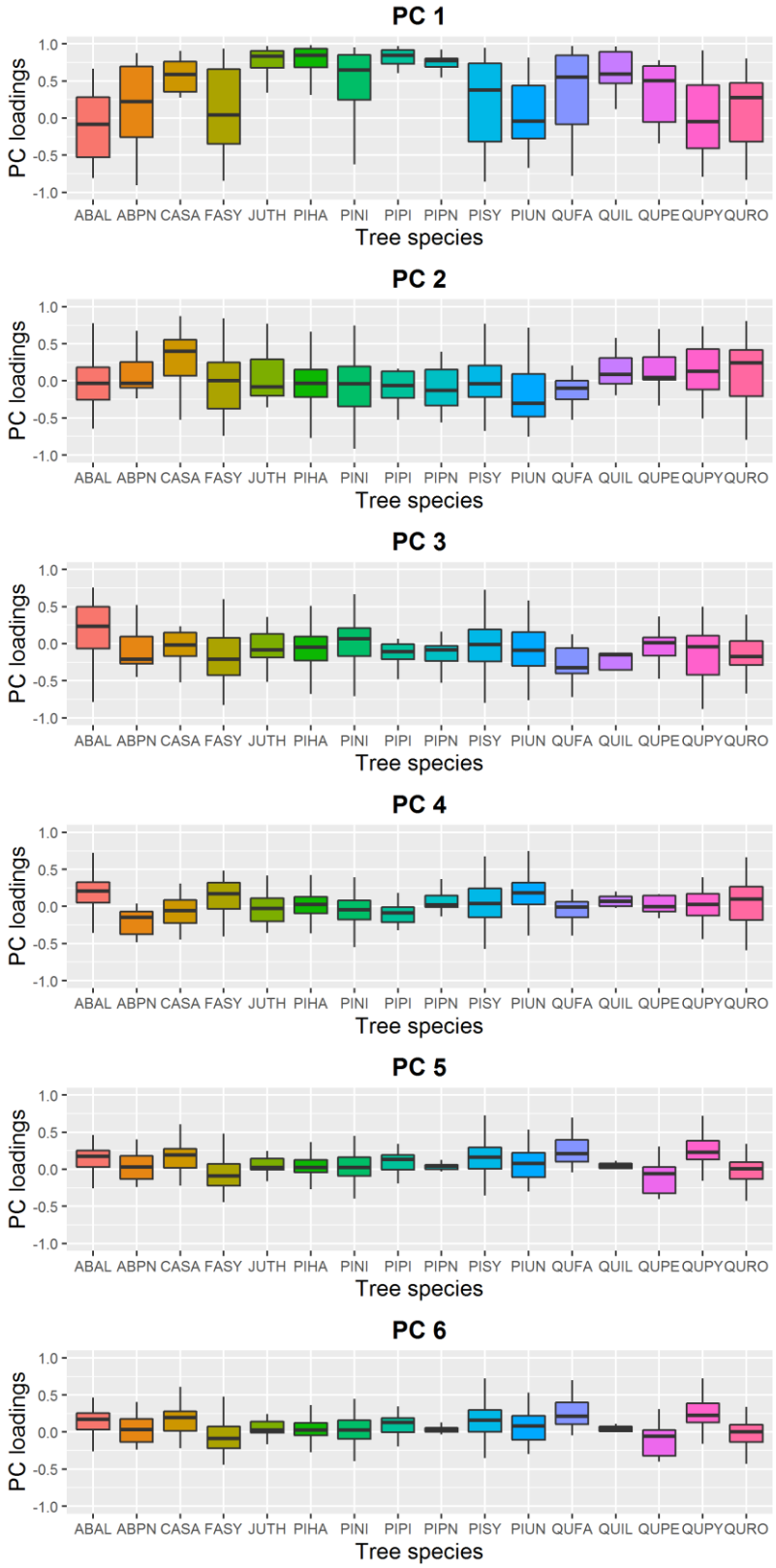

Figure 5. Box plots showing PC loadings for the different tree species. For each box plot, the central solid line indicates the median. The whiskers represent the 10th and the 90th, while the 25th and the 75th are plotted as the vertical lines of the bounding boxes. All codes of species correspond to those listed in Table 1.